Microchemical Journal 222 (2026) 117195

Contents lists available at ScienceDirect

Microchemical Journal

journal homepage: www.elsevier.com/locate/microc

Development of polysulfone bead/NH_2-MIL-101 (Cr) as new sorbent in the pipette tip micro-SPE method for the determination of pesticides in water and food samples

Soleen Burhan Ahmed [a], Soleyman Moinfar [b,c,*]

[a] Department of chemistry, college of science, university of Duhok, Duhok 42001, Iraq
[b] Chemical Analysis Research Centre, Scientific Research Centre, University of Zakho, Zakho, Iraq
[c] Department of Basic Sciences, College of Pharmacy, Nawroz University, Duhok, Iraq

ARTICLE INFO

Keywords:
Polysulfone beads/NH_2-MIL-101(Cr)
Pipette tip-micro solid phase extraction
HPLC-PDA
Pesticides
Well water
Food sample

ABSTRACT

This study developed and tested polysulfone (PSF) beads with NH_2-MIL-101(Cr) as a sorbent for PT-μ-SPE. Pesticides were extracted and identified using a high-performance liquid chromatography-photodiode array detector (HPLC-PDA) on real samples such as well water, tea, and honey. PSF beads/NH_2-MIL-101(Cr) were synthesized and characterized using X-ray diffraction (XRD), Fourier Transform Infrared Spectroscopy (FT-IR), thermal gravimetric analysis (TGA), and scanning electron microscopy (SEM). In addition, the kind and quantity of eluent, pH, and sample volume were studied and optimized. The response surface methodology (RSM) was used to create regression models with a central composite design (CCD). The PSF beads/NH_2-MIL-101(Cr) sorbent in PT-μSPE has a linear range of 0.7 to 100.0 μg/L. The suggested technique is highly reproducible, with RSD % (intra-day) values ranging from 2.5% to 3.5%. The technique detected pesticides in water and food samples at concentrations of 33.0–100.0 μg/L, with recovery rates ranging from 80.0% to 102.0%.

1. Introduction

Pesticides are chemicals used in agriculture, forestry, horticulture, and public places to increase crop output and manage pests to meet world food demand [1]. Pesticides used in agriculture damage the environment because of their persistence, non-biodegradability, ability to accumulate, and lipid solubility, presenting a serious threat to human health and ecosystems. Moreover, certain pesticides have significant mobility in the environment, leading to contamination of air, soil, food, and drinkable water [2–4]. As a result, a number of countries have enacted rules that limit the use of certain pesticides in agriculture, such as maximum residue limits (MRLs). For example, the European Union (EU) has set a consistent MRL of 0.01 mg/kg for a number of pesticides [5]. Among pesticides, neonicotinoids (NEOs) are one of the most recent categories of synthetic insecticides, developed over the past three decades. NEOs are easily absorbed by plant tissues, leading to prolonged residual effects in agriculture [6]. Thiacloprid and acetamiprid are two neonicotinoid compounds widely used in agriculture [7]. Their unique properties make them the most commonly used NEOs, including high binding affinity for insect nicotine receptors of acetylcholine (nAChRs), low hydrophobicity, and high penetrability [8]. Furthermore, the half-life of acetamiprid has been estimated to be 25.1 days in soil under sunlight and the half-life of thiacloprid has been reported to be 9–16 days in soil under field conditions [8].

The development of rapid, reliable, and highly sensitive methods for determination of trace pesticide residues is essential due to the scarcity of pesticide residues in food and environmental samples [9,10]. A simple review of the literature indicated a wide range of research on the extraction and identification of pesticides in different samples, including dispersive liquid-liquid micro-extraction (DLLME) [11,12], magnetic solid-phase extraction (MSPE) [13], solid phase extraction (SPE) [14,15], micro solid phase extraction (μSPE) [16], liquid- phase microextraction (LPME) [17], solid-phase micro extraction (SPME) [18], and dispersive micro solid phase extraction (DMSPE) [19] which are among the most frequently used extraction methodologies in this field. However, all these techniques show certain practical limitations. For example, organic solvents, which are frequently hazardous, are employed as extractants during LPME procedures. This hazardous organic solvent is utilized in small quantities; however, it has the capacity to bioaccumulate and penetrate ecosystems, leading to

* Corresponding author at: Chemical Analysis Research Centre, Scientific Research Centre, University of Zakho, Zakho, Iraq.
E-mail address: soleiman.moeinfar@uoz.edu.krd (S. Moinfar).

https://doi.org/10.1016/j.microc.2026.117195
Received 1 November 2025; Received in revised form 2 January 2026; Accepted 29 January 2026
Available online 30 January 2026

concentrations that surpass permissible limits. Furthermore, they frequently encountered challenges during the clean-up of food samples. As a result, they ultimately had a negative impact on the environment [20]. Environmental and dietary samples are frequently analyzed using the SPME, a solvent-free and straightforward extraction method. T.-T. Ma et al. [21] observed many problems in commercially available fibers, including extended extraction durations, insufficient thermal stability, limited solvent resistance, restricted adsorption capacity, poor durability, and brittleness. Presently, solid-phase extraction (SPE) methodologies predominantly serve as a sample preparation technique, particularly in cartridge mode, for aqueous matrices, the preconcentration of pesticides, and the clean-up of food samples [22,23]. The conventional SPE method is limited by many disadvantages, such as excessive solvent consumption, expensive cartridges, and intricate procedures [24]. One of the attractive SPE techniques that uses MOF as an adsorbent for the extraction of pollutants is the magnetic solid-phase extraction method [25]. Although in the recent few years, various MOF composites have been investigated as effective adsorbents in MSPE method such as Magnetic porous carbon nanocomposite derived from cobalt-MOF and magnetic nano-composite derived from MMIL-88 A [26,27]. However, due to the need to disperse and collect the adsorbent in food samples, the possibility of loss of the adsorbent and the target analyte increases. Consequently, this study used pipette tip micro-solid phase extraction (PT-μSPE). This method has recently been employed as an alternative to conventional SPE for the pre-concentration of compounds from complex matrixes. It is highly promising. The approach offered distinct advantages, including cost-effectiveness, lower detection limits, minimal use of organic solvents, faster extraction (without shaking and centrifuge), and greater simplicity compared to traditional SPE cartridges [28]. However, the PT-μSPE is restricted by several factors, including the establishment of back pressure due to the adsorbent's properties and packing issues that arise when the sorbent is micro- and nano-scale particulates [29]. Consequently, the chemical and physical properties of sorbent are the essential factors to achieve higher enrichment factors and acceptable recoveries in SPE and micro-SPE [30]. Metal-organic frameworks (MOFs) are a novel class of adsorbents that have garnered significant attention in recent years. MOFs are a new category of porous materials that are composed of organic linkers and metal ions or metal clusters. The diverse varieties of these adsorbents are the result of the numerous methods of combining metals and ligands. This resulted in the development of a distinctive category of crystalline porous material [31,32]. MOFs are a remarkable choice for use as sorbents in SPE methodologies, as per [29]. This is due to their crystalline framework, high porosity, large specific surface area, tunable compositions, and structural parameters. However, the direct packaging of MOFs in PT-μSPE as a sorbent is accompanied by a variety of challenges, including an excessive extraction duration, obstruction, and increased packed-pipette tip back pressure [33]. Building a bulk MOF-polymer inside a polymer monolith support may overcome restrictions [33,34]. The insertion of nano- or micro-particles into organic polymer monoliths is a promising method for developing hybrid monolithic materials that incorporate the benefits of both material categories [34]. Various procedures were established to produce MOF-polymer monoliths for use in SPE devices [35]. The majority relied on including MOFs into the polymerization mixture, leading to materials with decreased MOF accessibility for analyte [36]. This approach was used in the field of chromatography [37]. However, it has seldom been examined due to sample treatment considerations [38]. HPLC pumps are needed to propel the sample solution through the monolithic polymer and the analyte's interaction with the MOFs particles in bulk polymer are limited. Consequently, a more efficient PT-μSPE method is necessary to eliminate back-pressure of the sample flow, increase the stability of the adsorbent and the contact area between the analyte and the MOFs. For the first time, this research proposed to solve this issue by using porous polymer beads containing MOFs on the surface and pores of the beads. In this study, we were selected polysulfone (PSF) to be supportive of MOFs particles, which are renowned for their thermal stability, chemical resistance, and mechanical strength across the pH wide range [39,40].

We synthesized NH_2-MIL-101(Cr) sorbent using the hydrothermal method in powder form. Next, for the first time, NH_2-MIL-101(Cr) particles are distributed in porous polysulfone beads. The primary benefits of spherical beads are reduced backpressure, prevent clogging, simple packing of pipette tips, and ease of eluting and reuse of the beads for several extraction. Furthermore, they are avoided MOFs agglomeration, reduced extraction time, and ensured stability in water and over a wide range of pH. In this study, for the first time, extraction of two distinct pesticides, namely acetamiprid, and thiacloprid, from well water and dietary samples (honey and tea) was implemented to, using PSF beads/NH_2-MIL-101(Cr) as an adsorbent in PT-μSPE method. Response surface methodology (RSM) is a statistical tool used to analyze and characterize the connection between a response variable and many inputs. Dependent variables represent the results, while independent variables denote the factors that affect the process. RSM analysis revealed a robust link between input and output variables. It provided optimal operational parameters for a system in the process of optimization or a parameter field that meets operational requirements. Central composite design is a pivotal experimental framework used in RSM [41,42]. Multiple practical factors such as pH, sample volume, desorption solvent volume, and desorption solvent type that influence extraction efficiency was evaluated and optimized by RSM. Whereas PSF beads/NH_2-MIL-101(Cr) functioned as the adsorbent, and the extracted pesticides were quantified by HPLC-PDA.

2. Materials and methods

2.1. Chemicals and materials

Kindly see the supplemental information (ESI) for specific information regarding the chemicals and materials.

2.2. Instrumentation

Kindly see the ESI for specific information regarding the instrumentation.

2.3. HPLC conditions

All studied pesticides were analyzed on an HPLC-PDA system (PerkinElmer, Flexar-15, USA). HPLC system equipped with a C18, 150 × 4.6 mm, 5 μm (Restek, USA) column and PDA (PerkinElmer, Flexar-15, USA), which was used for the separation and quantification of extracted insecticides at 244 nm. The HPLC conditions were initially selected based on a method previously published by our research group [43]. The final section of the elution program was then slightly modified to improve column washing and remove unwanted compounds. HPLC-grade water and acetonitrile were degassed and used as the mobile phase at a flow rate of 1.0 mL/min. Each sample contained 20.0 μL, was injected to HPLC using autosampler (PerkinElmer, USA). The mobile phase was composed of water (A) and acetonitrile (MeCN) (B). The gradient elution program was as follows: initial 21.0% B (for 1.0 min), to 27.0% B in 1.0 min and hold for 2.5 min, from 27.0% to 38.0% B in 3.0 min, from 38% to 60.0% B in 2.5 min, and hold in 60.0% 2.0 min, return to 21.0% B in 2.5. The total chromatographic time for a single run was 14.5 min.

2.4. Synthesis of NH_2-MIL-101(Cr)

The synthesis of NH_2-MIL-101(Cr) was followed the method explained by Moinfar and Khodayari [44]. Initially, a Teflon reactor was filled with eight mmol (3.20 g) of Cr $(NO_3)_3{\cdot}9H_2O$ and eight mmol (1.44 g) of 2-amino terephthalic acid. Then, 60.0 mL of 0.33 M NaOH was added in a dropwise manner. The solution was then homogenized by

stirring it at 700 rpm for 60 min. Following 16 h of heating to 160 °C, the reactor was returned to room temperature. The solid powder was isolated using a centrifuge operating at 7000 rpm for 15 min. The resulting powder was washed three times with deionized water. The samples were centrifuged for about 5.0 min at 7000 rpm after a wash with 30 mL of DMF (for 16 h). To eliminate DMF residue, MOFs were washed with 50 mL of methanol (reflux for 12 h). The processed powder was ultimately dried at 70 °C for approximately 12 h.

2.5. Synthesis of PSF beads and PSF beads/NH_2-MIL-101(Cr)

Initially, 0.6 g of PSF was dissolved in 4.0 mL of DMF with continuous stirring at 45 °C for 12 h to create a homogenous casting solution [45]. Subsequently, 0.15 g of NH_2-MIL-101(Cr) was added and mixed to achieve a homogeneous mixture. Beads were fabricated by injecting a mixture of PSF and NH_2-MIL-101(Cr) into deionized water using 2-mL syringe. In this step, the obtained PSF beads/NH_2-MIL-101(Cr) were immersed in deionized water for 24 h to eradicate any remaining DMF solvent. Afterward, the beads were rinsed with methanol for 6 h and subsequently desiccated in an oven at 100 °C for approximately 48 h.

2.6. Preparation of the pipette tip-μSPE

50.0 mg of PSF beads/NH_2-MIL-101(Cr) packed in a 1 mL pipette tip. Then, prepared pipette tip was sequentially washed with 600 μL of MeCN and 1.0 mL of ultrapure water. The prepared tip was used for the extraction of target pesticides from samples.

2.7. Preparation of real samples

The collected Duhok well water sample was spiked with a certain amount of standard solution. Methanol was used to prepare the pesticide standard solution. After spiking the samples with the pesticide mixture, they were then run through a packed pipette tip and examined in compliance with section 2. 8. A final volume of 45.0 mL was achieved by diluting 5.0 g of honey-free wax with ultrapure water (40 °C). Then, spiked samples pH were adjusted to 6.0. Ultimately, section 2.8 was adhered to throughout the extraction process. The following are the steps to prepare tea: 2.5 g of black tea was added to the beaker after being purchased at the local market. After adding 100.0 mL of boiling water, they were let to sit for about 15.0 min until they reached room temperature. The pesticides standard solution was then added in a predetermined quantity and stirred. To exclude extra seeds, pulp, and herbs from the tea, the matrix solutions were centrifuged for 10.0 min at 4100 rpm. Prior to analysis, the pH of each sample was determined and brought to 6.0. Ultimately, section 2.8 was adhered to throughout the extraction process.

2.8. Extraction procedure

The first, sample's pH had been adjusted to 6.0 using a 0.1 M HCl and 0.1 M NaOH solution. Next, 45.0 mL of spiked or blank samples were passed through the packed pipette tip holding the PSF beads/NH_2-MIL-101(Cr) at a flow rate of 3.0 mL/min. Then, the pesticides that had been adsorbed on the sorbent were subsequently desorbed using 175.0 μL of pure MeCN. After that, 20.0 μL of collected MeCN, which included extracted analytes, was injected to the HPLC-PDA. The beads in pipette tip were washed with 600.0 μL of MeCN and 1.0 mL of ultrapure water after each extraction, to be free of any probably contamination for the next extraction.

2.9. Experimental design

Employing statistical techniques and a response surface methodology to reduce chemical waste, enhance experimental efficiency, and decrease overall costs [46]. To optimize the enrichment factor and achieve optimal extraction conditions for acetamiprid, and thiacloprid, many parameters influencing PT-μSPE were selected and analyzed. Thus, the PT-μSPE approach was affected by four parameters. The parameters included the volume of the desorption solvent (140.91, 175.0, 225.0, 275.0, and 309.09 μL), the sample volume (15.0, 21.0, 30.0, 38.0, and 45.0 mL), the type of desorption solvent (methanol, MeCN, and a methanol-MeCN combination), and the pH levels (3.5, 4.7, 6.5, 8.2, and 9.5). We generated a matrix with 54 experimental runs (Table S1) by putting the desorption solvent type into a category variable and the three parameters (pH, sample volume, and desorption solvent volume) into numerical variables. The model design is a reduced cubic, optimized using Design Expert software version 13.0.5. For response elution, we utilized the peak area derived from HPLC-PDA results. The results of pesticide adsorption were presented by the analysis of variance (ANOVA) and illustrated in a three-dimensional graph.

3. Results and discussion

3.1. Characterization

3.1.1. SEM analysis

Scanning electron microscopy (SEM) is used to show the surface morphology of NH_2-MIL-101(Cr) in Fig. S1. The stable octahedral crystal structure of NH_2-MIL-101(Cr) supports the conclusions of [47]. The resulting NH_2-MIL-101(Cr) has octahedral microcrystals with edges that are, on average, between 154.5 and 319.3 nm long. A sphere with a diameter of around 2 mm is the PSF beads that is produced. Fig. 1 (a and b) shows the cross-section of the PSF beads and the PSF beads/NH_2-MIL-101(Cr). Fig. 1a shows the particle's huge, wide channels and porous features, which are the outcome of PSF beads. PSF beads structure facilitates high permeability and sample rapid flow during extraction, which NH_2-MIL-101 (Cr) on the surface and within the pores of PSF beads was doped. As Fig. 1c seem to be smooth on the PSF beads' surfaces. In contrast, Fig. 1d shows that the Cr-MOFs are evenly dispersed throughout the surface of the PSF beads and penetrated to pores.

3.1.2. XRD analysis

Fig. 2a displays the XRD patterns of NH_2-MIL-101(Cr), PSF beads, and PSF beads/NH_2-MIL-101(Cr) at 5–80 Å. XRD pattern for NH_2-MIL-101(Cr) reveals typical peaks at 2θ values of 9.03°, 16.72°, 24.92°, and 42.77°, which are consistent with previous studies [44]. The sharp diffraction peaks indicate that the synthesized Cr-MOF is highly crystalline, illustrating the successful construction of NH_2-MIL-101(Cr). The XRD pattern of PSF exhibits a diffraction peak at 2θ of 17.18° (Fig. 2a), indicating that the polymer phase is predominantly amorphous. The XRD profile of PSF beads/NH_2-MIL-101(Cr) showed both sharp peaks consistent with crystalline MOFs and broad peaks confirming the amorphous nature of PSF. These broad peaks, indicating the incorporation of MOFs in PSF beads, cause a slight increase in polymer chain disorder. Furthermore, the PSF had only a tiny impact on the reduction in MOF crystallinity.

3.1.3. Thermal gravimeter analysis (TGA) interpretation

Fig. 2b compares the thermal stability of NH_2-MIL-101(Cr), PSF, and PSF beads with NH_2-MIL-101(Cr). The curve was developed in an air environment ranging from 50 to 1050 °C at a rate of 10 °C per minute. The NH_2-MIL-101(Cr) thermogram reveals three distinct weight losses for this molecule. The first weight loss of 8% occurred at temperatures ranging from 50 to 87 degrees Celsius. This is induced by the evaporation of water adsorbed on the surface and inside the huge pores of NH_2-MIL-101(Cr). The second loss (6%) occurred between 100 and 220 °C, when the organic solvents and residual 2-aminoterephthalic acid that may have been confined between the smaller pores were eliminated, resulting in the presence of only the NH_2-MIL-101(Cr). The weight loss was 64% from 228 to 335 °C as a result of the thermal degradation of 2-aminoterephthalic acid coordinated with chromium oxide clusters. The

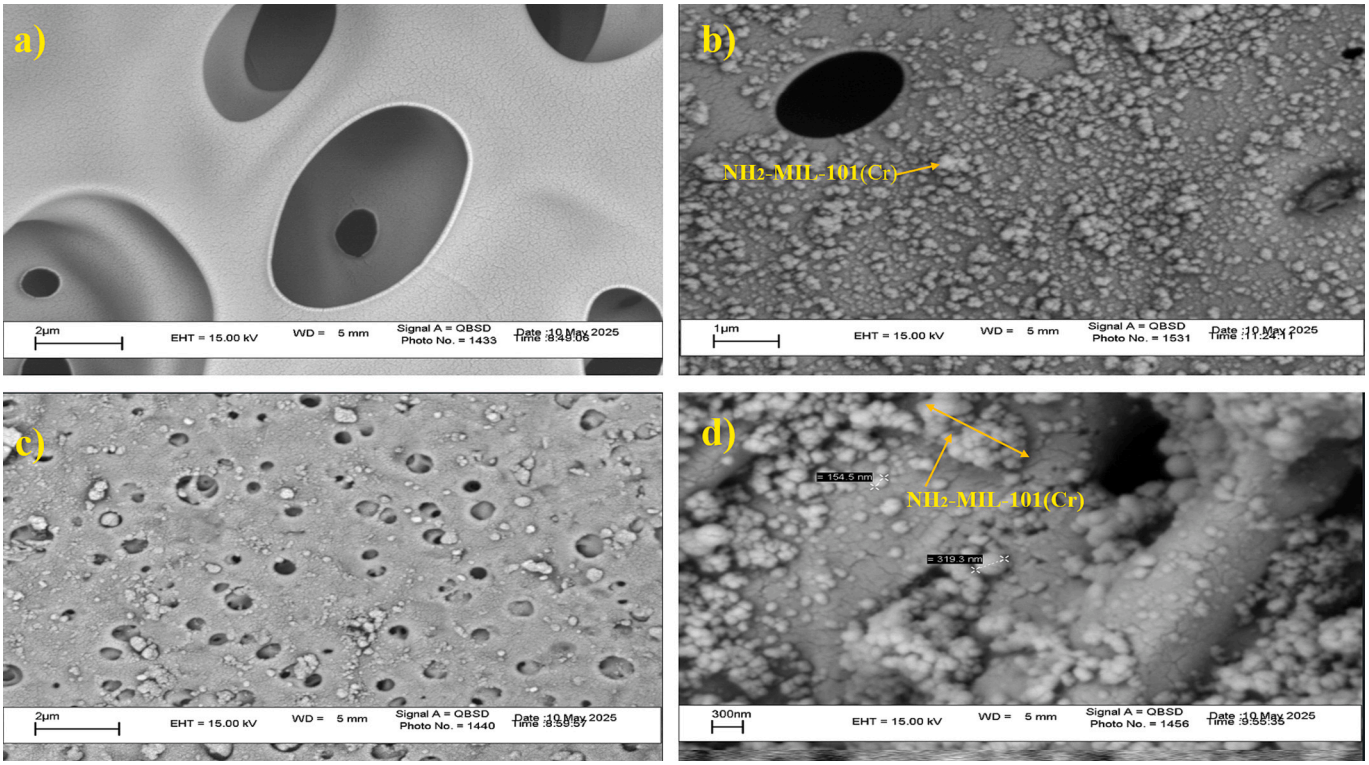

Fig. 1. SEM images of cross-section are (a -b), where (a) is for PSF beads and (b) is for PSF beads/NH_2-MIL-101(Cr). SEM images of the surface are (c-d), where (c) is for PSF beads and (d) is for PSF beads/NH_2-MIL-101(Cr).

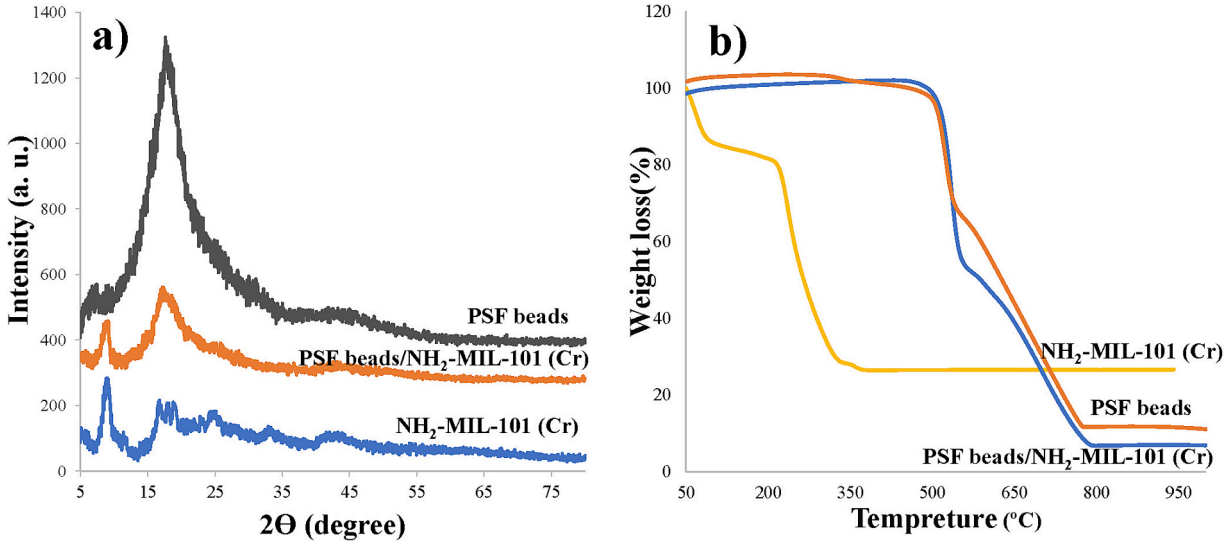

Fig. 2. (a) XRD pattern of NH_2-MIL-101(Cr), PSF, and PSF beads/NH_2-MIL-101(Cr) and (b) TGA pattern of PSF beads/NH_2-MIL-101(Cr), PSF, and NH_2-MIL-101(Cr).

sample's ultimate residual weight was 26% of its initial weight at 670 °C, which may be attributed to chromium oxide [48]. The PSF polymer exhibited a high degree of thermal stability, as evidenced by Fig. 2b, with a degradation temperature of approximately 530 °C [49]. The TGA curve for the PSF beads/NH_2-MIL-101(Cr), shown in Fig. 2b, demonstrated stability over the temperature range of 100 to 500 °C. A 42% weight reduction between 500 and 550 °C indicates the characteristic thermal degradation of polysulfone, particularly involving the loss of sulfonic groups from the polymer chains [50]. Fast breakdown transpires between 560 and 800 °C, leading to about 48% weight loss, which signifies the degradation of polysulfone and perhaps some Cr-MOF. At temperatures over 800 °C, around 10% of the mass is stabilized, perhaps attributable to the presence of chromium in NH_2-MIL-101(Cr). This confirms that the MOFs were uniformly distributed in the polysulfone solution. The DTG curve of PSF beads/NH_2-MIL-101(Cr) demonstrates superior thermal stability relative to pure NH_2-MIL-101(Cr). This may be attributed to the high thermal resistance of PSF used in the production of PSF beads/NH_2-MIL-101(Cr).

3.1.4. FT-IR analysis

To verify the successful reaction of polysulfone with NH_2-MIL-101 (Cr), the FT-IR spectra of the metal-organic frameworks, including the

parent NH_2-MIL-101(Cr), polysulfone, and polysulfone beads/NH_2-MIL-101(Cr) samples, were compared, as illustrated in Fig. S2. The stretching vibration of Cr—O is indicated by the substantial peak at 535 cm^{-1} in the spectrum of NH_2-MIL-101(Cr). The peaks at 1388 cm^{-1} confirm the existence of amino groups. The addition of amine groups to the NH_2-MIL-101(Cr) is confirmed by the N—H stretching vibrations seen at 3401 cm^{-1} and 3305 cm^{-1} as well as a C—N stretch at 1259 cm^{-1} [51]. Peaks at 1570 cm^{-1} and 1107 cm^{-1} are attributed to C—C and C—H stretching within the benzene rings [52]. Additionally, O–C–O asymmetric stretching is observed at 1441 cm^{-1} and 1383 cm^{-1}. The bands at 1256 cm^{-1} and 766 cm^{-1} correspond to C—N stretching and the vibrations of di-substituted aromatic rings, respectively [53]. The absence of strong signals between 1680 and 1720 cm $^{-1}$ indicates that the carboxyl (-COOH) groups in 2-aminoterephthalic acid are efficiently coupled with chromium ions, incorporating into the MOF structure [50]. The reformed sample exhibited bands in the FT-IR analysis of the PSF. The unique absorption peak at 1151 cm^{-1} in the PSF spectrum was attributed to the stretching vibration of O=S=O [54]. Peaks at 1504 cm^{-1} and 1242 cm^{-1} were attributed to the skeletal vibration of the aromatic ring and the stretching vibration of C-O-C, respectively [55]. PSF beads/NH_2-MIL-101(Cr) effective synthesis is confirmed by the FT-IR spectrum, which features all of the NH_2-MIL-101(Cr) characteristic peaks and overlaps with the PSF.

3.2. Optimization by central composite design

3.2.1. Optimization of extraction

The CCD approach in RSM methodology enables researchers to construct a suitable predictive relationship between the independent factors and the response variable [56]. Table S2 illustrates the implementation of CCD under RSM for three numerical factors and one categorical factor, each with five levels ($-\alpha$, -1, 0, $+1$, and $+\alpha$), in the current investigation. To (i) determine the optimal parameter values, (ii) identify variables that substantially influence peak areas, (iii) refine the peak areas of analytes, and (iv) investigate interactions, the CCD technique was implemented in this study. The experiment involved adjusting parameters, including pH (A), desorption solvent volume (B), sample volume (C), and desorption solvent type (D). This was done to conduct the CCD. The response for each pesticide was determined using the HPLC peak area of all analytes, as shown in Table S1. The Reduced Cubic model was employed to replicate all pesticide responses. The statistical analysis and mathematical model fitting of the experimental results regarding the adsorption of acetamiprid and thiacloprid are illustrated in Tables S4 and S5. The cubic model may provide a substantial explanation for the responses of the variables and their interactions, as indicated by the ANOVA results. The model F-value of acetamiprid demonstrated 357.05. Thiacloprid demonstrated F-values of 598.30. These findings suggest that the model is statistically significant for both analytes. The likelihood of an F-value this significant being the result of random noise is approximately 0.01%. The *p*-value of 0.0001 for all analytes confirms the significance of the cubic model terms, and a p-value of less than 0.0500 indicates the essentiality of the cubic model terms. The F-values for Lack of Fit are non-significant, which is advantageous for model fitting. In particular, the Lack of Fit F-value for acetamiprid was 0.54, and for thiacloprid it was 1.87. Compared with pure error, these values are not statistically significant. The precision and accuracy of the model were all confirmed by the coefficient of variation (C.V.%), standard deviation, and coefficient of determination, as shown in Table S5. The model's accuracy, dependability, and reproducibility were demonstrated by the results, which indicated that the C.V.% for the extraction of two pesticides was less than 10%. A substantial coefficient of variation, indicating substantial variation in the mean value, indicates an insufficient response model [57]. Adequate accuracy is one of the main parameters used to assess the quality of the selected cubic model for data fitting. A signal-to-noise ratio of "adequate precision" is defined as one that is more than 4. The signal-to-noise ratios of the two analytes ranged from 83.3814 to 112.077. This illustrates the model's capacity space and supports the statistical significance of the model that was generated. Table S5 displays the coefficient of determination (R^2), the predicted value, and the adjusted value. The operational factors under investigation accounted for 99.77% to 99.86% of the total variation, as indicated by the R^2 values for the two pesticides, which ranged from 0.9977 to 0.9986. This leads to a simple 0.14% to 0.23% of variation remaining unexplained. The small quantity of inexplicable variance served as evidence of the model's superior fit to the experimental data. In contrast, the adjusted R^2 for acetamiprid was 0.9890; however, the predicted R^2 was 0.9949. The adjusted R^2 value for thiacloprid was 0.9969, while the predicted R^2 value was 0.9911. As evidenced by the "Adjusted R^2" in Table S5, the experimental data were well-fitted to the model, and it is nearly identical to the "Predicted R^2". To optimize the critical factors and define the response surface in the experiment, the RSM was developed in the subsequent phase of the design, taking into account all relevant interactions in the CCD, as depicted in Fig. 3 (a) for acetamiprid and (b) for thiacloprid. The generated response surfaces for the design are shown and demonstrate the 3D response surface plots of key variables. The plots were created for designated parameters while keeping other variables at constant and ideal levels. The influence of A (pH), B (volume of desorption solvent), C (sample volume), and D (type of desorption solvent) on the extraction efficiency of the analyzed pesticides was evaluated within a defined range of variables, with results illustrated as three-dimensional surface response plots and contour plots. It demonstrated a significant link between the independent factors and their best response. The extraction of acetamiprid and thiacloprid was enhanced at a pH of 6.0 and with an increasing sample volume. A higher sample volume results in a greater amount of pesticides and, thus, a higher level of adsorption [44]. The sample volume was 45.0 mLwas chosen because it yielded a high extraction efficiency.

Fig. 3 shows that the optimal extraction efficiency was achieved at pH 5.0–7.0 for all examined insecticides. The pH of the sample solutions markedly affected extraction efficiency, the adsorption of analytes within the pores of MOFs, with the structure of MOF crystals, the charged species present, and the existing forms of the analytes [58]. Furthermore, pesticides are also affected by pH, which influences their hydrophobic and hydrophilic properties. At pH 7–9.5, extraction first reached a zenith but then diminished significantly, perhaps owing to the degradation of insecticides or the structural instability of the sorbent under very alkaline conditions [59]. A similar decrease was seen below pH 4.5, suggesting that pesticides are ineffective under significantly acidic or basic conditions. Therefore, the sample's pH was adjusted to 6.0 to achieve high extraction efficiency.

In addition, the properties of the organic solvent profoundly influence the desorption of analytes from the sorbent. Furthermore, the volume of extraction solvent also influences the extraction performance of analytes from the sorbent. The extraction effectiveness improves as the volume of the extraction solvent diminishes, this is mostly attributable to the constancy of the maximum analyte adsorption capacity on the sorbent surface. Consequently, any additional increments in the solvent volume will result in the dilution of the analyte, resulting in a diminished peak [30]. As a result, 175.0 μL of acetonitrile was used for the desorption of analytes from PSF beads/NH_2-MIL-101(Cr).

To evaluate the impact of solvent type on desorption, methanol, acetonitrile, and a mixture of methanol and acetonitrile were investigated. Acetonitrile produced the highest peak areas for the target pesticides. This outcome can be explained by the solvent characteristics, acetonitrile is a polar aprotic solvent with a higher dielectric constant compared to methanol, which allows to disrupted of hydrogen bonding and π-π interaction between analyte and sorbent [30], therefore acetonitrile was selected as the desorption solvent in subsequent experiments.

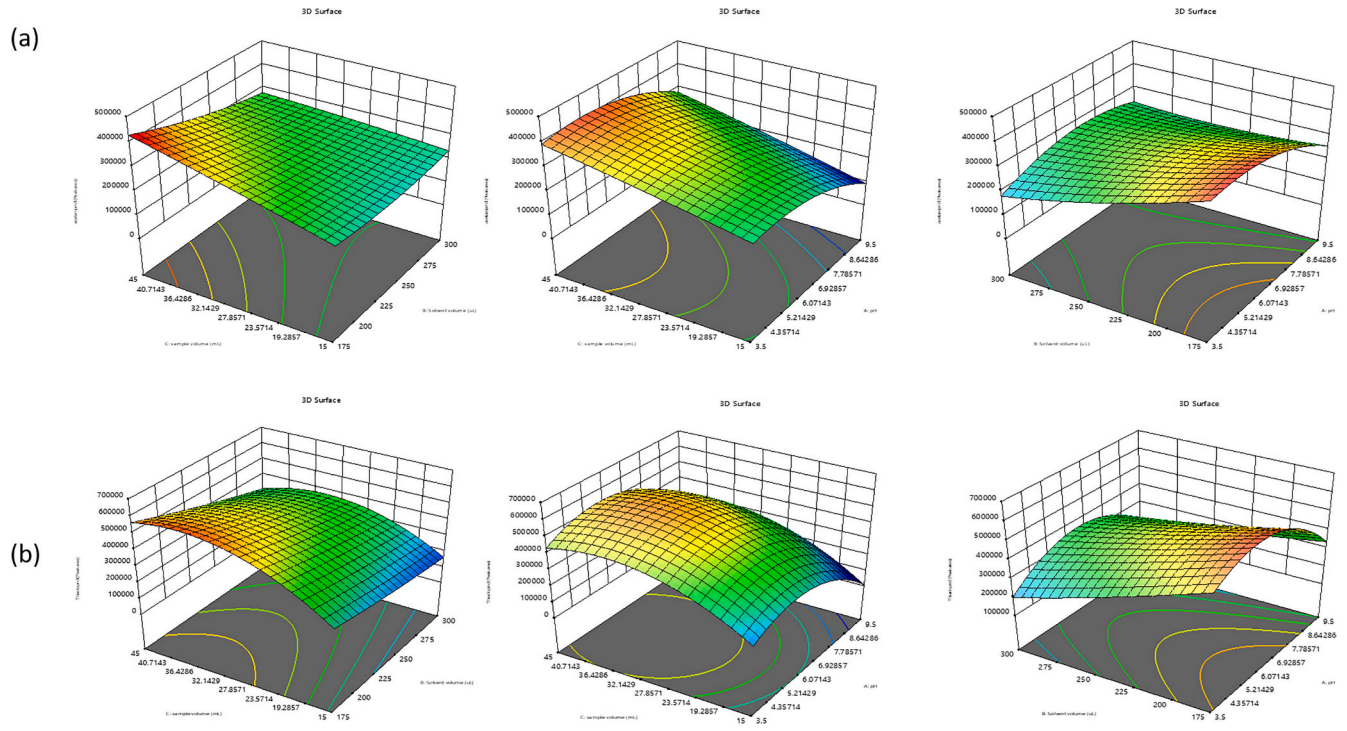

Fig. 3. The results obtained for the interaction between parameters using Design Expert software (a) for acetamiprid (b) for thiacloprid. The 3D plot of pH, sample volume, type, and volume of desorption solvent interaction.

3.3. Determination of the point of zero charge pH (pH_{pzc})

The point of zero charge (pH_{pzc}) denotes the pH at which the net charge of solid surface particles is neutral. At pH_{pzc}, the amounts of acidic and basic functional groups in sorbents are equal. Below the point of zero charge (pH_{pzc}), sorbents exhibit a positive net charge and preferentially adsorb anionic species; conversely, beyond the pH_{pzc}, cationic entities are preferred [60]. The immersion approach was used to determine the pH_{pzc} for the (PSF beads/NH_2-MIL-101(Cr)). We made 10 solutions, each having 7.0 mL of 0.1 M sodium nitrate. The pH of each solution was between 2.0 and 11.0, and we changed the pH by adding 0.01 M NaOH and 0.01 M HCl. Then, 50.0 mg of the beads were added to each solution, and the mixtures were agitated for 24 h. The pH of each solution was rechecked. The difference between the initial pH (pHi) and the final pH (pHf) was calculated, and the results were plotted against the pHi, as shown in Fig. S3. The produced beads have a pH_{pzc} of 4.8, resulting in a ΔpH value of 0. At pH levels below 4.8, the beads have a positive net charge, which aids in the adsorption of anionic pesticides; at pH levels above 4.8, the bead's negative net charge makes it more vulnerable to the absorption of cationic pesticides. The research determined that the optimal pH was 6.0. In a pH setting above 4.8, PSF beads/NH_2-MIL-101(Cr) had a negative net charge, which aided cationic pesticide adsorption. It is important to maintain mild acidic to neutral pH levels (pH ~ 6.0) in order to maximize acetamiprid's adsorption ability. Because of the electrostatic repulsion force between the acetamiprid molecules and the adsorbent, the extraction efficiency decreases as the pH rises. In a highly acidic medium, the extraction efficiency of the synthesized MOFs decreased due to their potentially hydrolytic nature at a very low pH (pH = 2.0) [61]. Additionally, the charge of thiacloprid was positive when pH was less than 4.0. In the present investigation, we discovered that the adsorbent has a positive charge when the pH is less than 4.8. Consequently, the electrostatic repulsion leads to a reduction in extraction efficiencies. The extraction efficiencies of the two analytes decrease as the pH value exceeds 8.0, as a result of the increased interaction between the anionic OH- species in the sample solution and the thiacloprid cationic-π bonding [62]. Consequently, the two analytes demonstrate an optimal pH of 6.0.

3.4. Comparison of the extraction efficiency of different amounts of MOFs in PSF beads

We synthesized polysulfone beads with varying percentages of MOFs (pure PSF, PSF beads/NH_2-MIL-101(Cr) 13%, PSF beads/NH_2-MIL-101 (Cr) 26%, and PSF beads/NH_2-MIL-101(Cr) 50%) to assess the impact of MOF quantity on extraction efficacy. Subsequently, we packaged the beads into pipette tips. The maximal peak area of each pesticide was determined after extraction under identical conditions. The extraction efficiencies of all examined pesticides were improved by PSF beads/NH_2-MIL-101(Cr) 50%, as illustrated in Fig. 4a. Especially at 50.0%, this must indicate a greater availability of active adsorption sites and improved pore accessibility within the polysulfone matrix. As the proportion of MOF rises, the total surface area accessible to the analyte expands, resulting in an increase in adsorption interactions (hydrophobic, π-π, or hydrogen bonding) [63]. Loading the MOF beyond 50% wasn't done due to insufficient homogeneity of the composite. Increased MOF concentrations resulted in irregular dispersion and particle agglomeration, potentially compromising the structural integrity of the composite and the consistency of the extraction performance.

3.5. Figures of merit

The performance metrics of PT-μSPE utilizing PSF beads/NH_2-MIL-101(Cr) as sorbent, including limit of detection (LOD), limit of quantification (LOQ), linearity range (L.R), relative recovery (RR), inter-day and intra-day relative standard deviation (RSD%), and enrichment factor (EF), are presented in Table 1. The reproducibility of the suggested approach for PSF beads/NH_2-MIL-101(Cr)-PT-μSPE was assessed by five duplicate experiments using water samples containing 66.0 μg/L of each analyte. The inter-day accuracy of PSF beads/NH_2-MIL-101(Cr) - PT-μSPE was assessed using three duplicate tests conducted over three days, maintaining the sorbent unchanged [30]. Minimal RSD % percentages were noted for the various pesticides (maximum 3.4%), indicating that

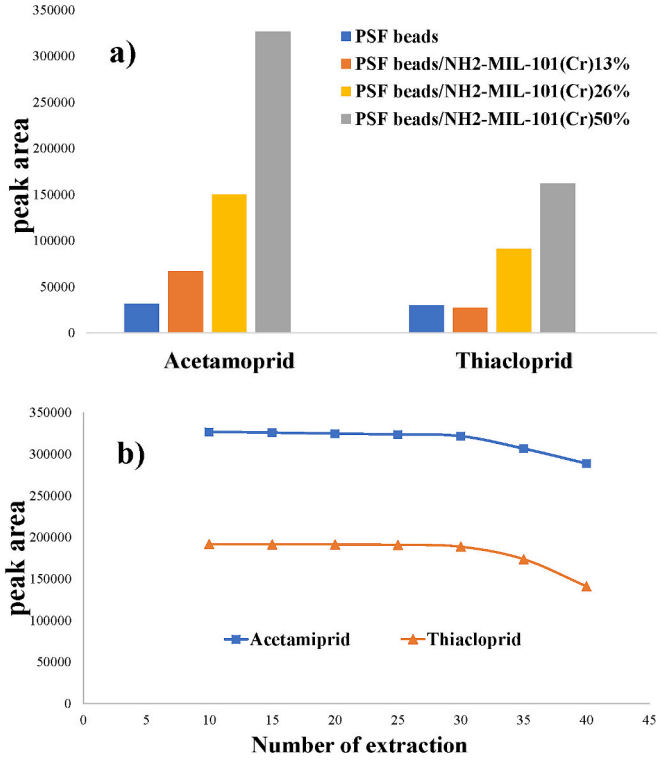

Fig. 4. (a)Comparison of the extraction efficiency of different amounts of Cr-MOF in PSF beads and (b): Extraction performance of the PSF beads/NH_2-MIL-101(Cr) adsorbent across 40 reuse cycles, evaluated using HPLC-PDA detection of acetamiprid and thiacloprid.

the method's precision is suitable for the analysis of the pesticides examined. Table 1 illustrates that the favored methodology demonstrated a R^2 value of 0.99 and a linear range of 0.7–100.0 μg/L. By analyzing chromatograms with a signal-to-noise ratio of three [64], the LODs for the PT-μSPE method with respect to pesticides in water samples were determined, resulting in values ranging from 0.2 to 0.3 μg/L. LOQ (S/N = 10) [64] was 0.7–1.0 μg/L. The EFs were determined by employing the following equation, where C_{aq} represents the analyte concentration in the original solution and C_{org} represents the analyte concentration in the desorption solvent following PT-μSPE [65].

$$EF = \frac{C_{org}}{C_{aq}}$$

3.6. Reusability

The synthesized PSF beads/NH_2-MIL-101(Cr) stability was evaluated throughout 40.0 cycles of extraction under optimum conditions. PT-μSPE was employed with acetamiprid and thiacloprid concentrations of 66.0 μg/L to assess the extraction. The performance of the reused sorbent following these cycles. Fig. 4b illustrates that the extractability of acetamiprid and thiacloprid utilizing the beads, PSF beads/NH_2-MIL-101(Cr) remained mostly unchanged up to 30.0 cycles, followed by a declining trend afterward, as determined by HPLC-PDA adsorption of acetamiprid and thiacloprid. This demonstrates that the synthesized adsorbent exhibits excellent stability under the optimized experimental conditions.

3.7. Matrix effect

The matrix effect (ME%) was studied by comparison of analytical signal obtained in spiked ultra-pure water and spiked samples. The following equation then calculates the matrix effect (ME) [30]:

$$ME\% = \frac{As - An}{Aw} * 100$$

whereas A_s, A_n and A_w are the peak areas of analytes in the spiked real sample, un-spiked real sample and spiked ultra-pure water, respectively. As demonstrated in Table 2. The matrix did not significantly influence the analysis of analytes in water and tea samples; However, in more complex sample, such as honey, the matrix has a very small effect (89–94%), which is within acceptable range. To assess the method selectivity, potential interferences from chemicals that may coexist with the analytes were examined in accordance with the guidelines of the US Food & Drug Administration (FDA) Guidelines for method validation [30]. Fig. 5 illustrates that no significant interfering signal was detected in the chromatogram of the blank well water sample. Exhibiting excellent selectivity and appropriate chromatographic separation of NEOs (Fig. 5).

3.8. Real sample analysis

The current study was conducted to determine two pesticides in well

Table 2
Obtained tea, honey, and well water samples recoveries using a modified PT-μSPE-HPLC-PDA technique.

Water						
Analytes	Thiacloprid			Acetamiprid		
Spiked (μg/L)	0	33.0	100.0	0	33.0	100.0
Founded (μg/L)	2.4	33.7	92.6	nd	32.5	98.8
RR%	–	94.8	92.6	–	98.5	98.8
ME%	98.0%			99.0%		
Tea						
Spiked (μg/L)	0	33.0	100.0	0	33.0	100.0
Founded (μg/L)	nd	30.7	94.6	nd	31.4	102.9
RR%	–	93.0	94.6	–	95.2	102.0
ME%	94.0%			96.0%		
Honey						
Spiked (μg/L)	0	33.0	100.0	0	33.0	100.0
Founded (μg/L)	nd	26.4	94.7	nd	30.8	96.0
RR%	–	80.2	94.7	–	93.3	96.0
ME%	89.0%			94.0%		

Table 1
Analytical performance of the two insecticides in the water sample obtained.

Analytes	LOD(μg/L)[a]	LOQ(μg/L)[b]	L.R(μg/L)[c]	RSD% (intraday)[d]	RSD%(inters day)[e]	R^2[f]	EF[g]
Thiacloprid	0.3	1.0	(1.0–100.0)	3.4	5.7	0.99	210
Acetamiprid	0.2	0.7	(0.7–100.0)	2.5	3.8	0.99	200

[a] Limit of detection (S/N = 3) (μg/L).
[b] Limit of quantification(S/N = 10) (μg/L).
[c] Linear range (μg/L).
[d] Relative standard deviation at a concentration of 66.0 μg/L for each analyte for intra-day (n = 5).
[e] Relative standard deviation at a concentration of 66.0 μg/L for each analyte for inter-day (n = 3).
[f] coefficient of determination.
[g] Enrichment factor.

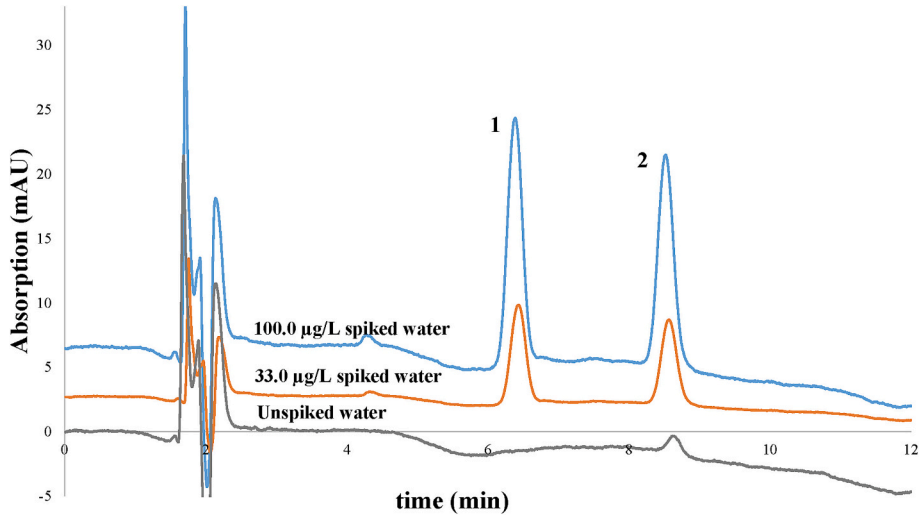

Fig. 5. The PT-µSPE-HPLC-PDA chromatograms of pesticides in unspiked and spiked water were extracted by PSF beads/NH_2-MIL-101(Cr). 1: acetamiprid. 2: thiacloprid.

water, tea, and honey to estimate method capability for real sample analysis. To assess the accuracy of the current method, the samples were spiked with different quantities of the pesticides (33.0 and 100.0 µg/L) and subjected to HPLC-PDA analysis. Table 2 provides a summary of the analytical findings. The accuracy of the suggested approach for identifying the pesticides in real samples was validated by the relative recoveries, which ranged from 93.0 to 102.0%. The chromatograms of pesticides extracted by PSF/NH_2-MIL-101(Cr) beads from un-spiked and spiked water samples are presented in Fig. 5. well water blank sample, 33.0 and 100 µg/L spiked well water samples chromatograms were displayed in Fig. 5. Fig.S4 and Fig.S5 are for honey and tea, respectively.

4. Comparison study

Various techniques were reported for pesticide extraction. Table 3 contrasts the results of the extraction of pesticides using this stated method with those of other popular methods. The accuracy of PT-µSPE-HPLC-PDA utilizing PSF beads/NH_2-MIL-101(Cr) as a sorbent was equivalent to alternative approaches. However, the suggested approach requires less extraction time and fewer organic solvents than other methods. Thus, the current method is appropriate for assessing pesticides in real samples. Table 3 shows the linearity range. The values obtained through our analysis are either equivalent to or more effective than those reported in prior research. Additionally, the current procedure provided a variety of benefits, such as the ability to re-use the packed pipet tip and a decrease in backpressure. Additionally, the efficiency of the proposed method is nearly equivalent to or superior to that of other reported methods.

5. Conclusion

Up to our knowledge, PT-µSPE has fewer problems than other sample preparation techniques, has numerous advantages, such as simplicity, low solvent consumption, minimal adsorbent requirements, portability, remarkable extraction efficiency, and very low cost. However, PT-µSPE has significant drawbacks, such as difficulties in preparing pipette tips when packing the sorbent in micro- and nano-scale particles, and production of backpressure owing to the adsorbent properties. As a result, it is vital to use support material to address this problem. Polysulfone beads were used as support material and encapsulated in PT-µSPE. Pesticide residues in well water, tea, and honey samples were measured using packed polysulfone beads/NH_2-MIL-101(Cr) in a pipette tip as a sorbent. Polysulfone also promoted the adsorption of target analytes, contradicting our earlier assumption and increasing adsorption and extraction efficiency. RSM properly adjusted the pesticide adsorption process variables to evaluate the effects of experimental parameters such as pH, sample volume, desorption solvent type, and desorption solvent volume. Two distinct pesticides were evaluated using the suggested approach, and the results showed high reproducibility and low detection limits. Furthermore, many more research might be conducted to investigate the influence of different polymers in conjunction with various other nanomaterials as sorbents for packing pipette tips in the extraction of diverse analytes. The structure of beads and their pores can have a significant effect on the availability of nanomaterials and extraction efficiency. Despite the several advantages of this method, several limitations should be noted: the outer layer of the PSF beads containing the MOF has much smaller and fewer pores than the inner part of the beads,

Table 3
Comparison of the current method with other reported methods for analyzing pesticides.

Method	Sorbent	Sample	LOD (µg/L)	RR	RSD%	L.R. (µg/L)	Extraction time (min)	Solvent (mL)	Ref.
HPLC-DAD	MIL-53(Al) MMM	water	0.013–0.064	80–119	3.62–12.78	0.04–15.0	35	10	[62]
MSPE-GC-FPD	G-SiO2-Fe3O4	Water	16–33	89.3–117.2	0.4–10.0	50–5000	7	6	[66]
SPMEHPLC-DAD	MOCP	Honey	0.05–0.15	91.5–103.5	5.4–8.8	0.5–600	25.30	1	[67]
SPE-HPLC-DAD	AuNPs-NH_2(C4)-ZIF-8	Agricultural samples	0.019–0.041	80–110	6.8–9.6	1–1000	20	2	[68]
PT-µSPE-HPLC-DAD	PSF beads-NH_2-MIL-101(Cr)	Tea, water, and Honey	(0.2–8)	82.27–102.91	2.5–5.9%	(0.7–200)	15.13	0.175	This study

MOCP: metal-organic coordination polymer.
AuNPs: gold nanoparticles.
MMM: Mixed Matrix Membranes.

as observed in SEM. This affected the extraction efficiency and reduced the accessibility of the analytes to the MOF adsorbent. Solving this problem could be the subject of further study.

CRediT authorship contribution statement

Soleen Burhan Ahmed: Writing – original draft, Validation, Software, Methodology, Investigation, Formal analysis. **Soleyman Moinfar:** Writing – review & editing, Validation, Supervision, Project administration, Investigation, Data curation, Conceptualization.

Declaration of competing interest

The authors declare that they have no known competing financial interests or personal relationships that could have appeared to influence the work reported in this paper.

Acknowledgments

The authors gratefully acknowledge the financial support of the University of Zakho and University of Duhok, Iraq.

Appendix A. Supplementary data

Supplementary data to this article can be found online at https://doi.org/10.1016/j.microc.2026.117195.

Data availability

No data was used for the research described in the article.

References

[1] G. Zhang, W.R. Kuesel, R. Olsson, R. Reed, X. Liu, B. Hopkins, Pesticide exposure patterns in honey bees during migratory pollination, J. Hazard. Mater. 480 (2024) 135910, https://doi.org/10.1016/j.jhazmat.2024.135910.
[2] P.P. Vázquez, C. Ferrer, M.J. Martínez Bueno, A. R., Fernández-AlbaPesticide residues in spices and herbs: sample preparation methods and determination by chromatographic techniques. *TrAC*, J. Trends Anal. Chem. 115 (2019) 13–22, https://doi.org/10.1016/j.trac.2019.03.022.
[3] S. Peng, L. Wang, L. Xu, Does farmland transfer promote green agricultural production? An empirical analysis of fertilizer and pesticide reduction, J. Clean. Prod. 489 (2025) 144631, https://doi.org/10.1016/j.jclepro.2024.144631.
[4] L.F. Viana, Occurrence of contaminants of emerging concern and their risks to the Pantanal Sul-Mato-Grossense aquatic biota, Brazil. Chemosphere 337 (2023) 139429, https://doi.org/10.1016/j.chemosphere.2023.139429.
[5] K. Weitzel, F. Chemie, M.S. Rev, Introduction, and C. Reference. Bond-dissociation energies of cations pushing the, WHO Libr. Cat. 30 (2) (2011) 221–235, https://doi.org/10.1002/mas.20276.
[6] K. Rawat, A. Srivastava, S. Tandon, G. Pal, Method validation for simultaneous determination of four neonicotinoids in vegetables by liquid chromatography, Anal. Sci. (2022) 0123456789, https://doi.org/10.1007/s44211-022-00227-y.
[7] M. Renaud, T. Akeju, T. Natal-da-luz, S. Leston, F. Ramos, Chemosphere Effects of the neonicotinoids acetamiprid and thiacloprid in their commercial formulations on soil fauna. 194 (2018) 85–93, https://doi.org/10.1016/j.chemosphere.2017.11.102.
[8] H.S. Lee, et al., Liquid chromatography–tandem mass spectrometry quantification of acetamiprid and thiacloprid residues in butterbur grown under regulated conditions, J. Chromatogr. B 1055 (2017) 172–177, https://doi.org/10.1016/j.jchromb.2017.04.021.
[9] M. Yeganeh, M. Farzadkia, A.J. Jafari, H.R. Sobhi, A. Esrafili, M. Gholami, Application of a magnetic solid-phase extraction method using a novel magnetic metal-organic framework nanocomposite for the extraction of malathion and diazinon pesticides from environmental water samples, Microchem. J. 183 (2022) 108082, https://doi.org/10.1016/j.microc.2022.108082.
[10] Y. Pang, X. Zang, H. Li, J. Liu, Q. Chang, S. Zhang, C. Wang, Z. Wang, Solid-phase microextraction of organophosphorous pesticides from food samples with a nitrogen-doped porous carbon derived from g-C3N4 templated MOF as the fiber coating, J. Hazard. Mater. 384 (2020) 121430, https://doi.org/10.1016/j.jhazmat.2019.121430.
[11] Y. Wang, X. Miao, H. Wei, D. Liu, G. Xia, X. Yang, Dispersive liquid-liquid microextraction combined with gas chromatography-mass spectrometry for the determination of multiple pesticides in celery, J. Food Anal. Methods 9 (2016) 2133–2141, https://doi.org/10.1007/s12161-015-0390-5.
[12] S. Chen, Y. Jiang, J. Li, M. You, R. Zhang, J. Li, Z. Fu, J. Xie, Z. Wang, In situ formation of solidified supramolecular solvent based dispersive liquid-liquid microextraction for the enrichment of phenylurea herbicides in water, fruit juice, and milk, Food Chem. 450 (2024) 139298, https://doi.org/10.1016/j.foodchem.2024.139298.
[13] Y. Wang, J. Li, P. Ma, D. Gao, D. Song, Synthesis of in-situ magnetized MOF-cellulose membranes for high-efficiency enrichment of diamide insecticides in vegetables and determination by LC-MS/MS, Talanta 270 (2024) 125626, https://doi.org/10.1016/j.talanta.2024.125626.
[14] P. Cliville-Cabre, L.M. Rosendo, F. Borrull, C. Aguilar, M. Calull, A comparative study of SPE-and DLLME-based methods for the determination of opioids and benzodiazepines in urine samples using LC–MS/MS, Microchem.J 208 (2024) 112354, https://doi.org/10.1016/j.microc.2024.112354.
[15] H. Zhou, Q. Shan, L. He, M. Zhang, C. Zhao, G. Zheng, L. Li, F. Xu, L. Ma, Y. Yin, Simultaneous determination of enantiomer residues of metalaxyl and its metabolite metalaxyl acid in animal muscle tissues by chiral liquid chromatography-tandem mass spectrometry, Food Chem. 435 (2024) 137599, https://doi.org/10.1016/j.foodchem.2023.137599.
[16] Z. Huang, K.H. Lee, Micro-solid-phase extraction of organochlorine pesticides using porous metal-organic framework MIL-101 as sorbent, J. Chromatogr. 1401 (2015) 9–16, https://doi.org/10.1016/j.chroma.2015.04.052.
[17] I. Timofeeva, A. Shishov, D. Kanashina, D. Dzema, A. Bulatov, On-line in-syringe sugaring-out liquid-liquid extraction coupled with HPLC-MS/MS for the determination of pesticides in fruit and berry juices, TalantaJ 167 (2017) 761–767, https://doi.org/10.1016/j.talanta.2017.01.008.
[18] M.M. Abolghasemi, S. Hassani, M. Bamorowat, Efficient solid-phase microextraction of triazole pesticides from natural water samples using a Nafion-loaded trimethylsilane-modified mesoporous silica coating of type SBA-15, Microchim. Acta 183 (2016) 889–895, https://doi.org/10.1007/s00604-015-1724-0.
[19] A.K. Ago, A.S. Kitte, A. Gure, Determination of organochlorine pesticides from juice samples using magnetic biochar-based dispersive micro-solid phase extraction in combination with dispersive liquid-liquid microextraction, Emerg. Contam J 10 (2024) 100283, https://doi.org/10.1016/j.emcon.2023.100283.
[20] H. Musarurwa, L. Chimuka, T.N. Tavengwa, Sorptive extraction of pesticides from food and environmental samples using metal organic framework-based adsorbents. *Trends environ*, Anal. Chem. 32 (2021) e00141, https://doi.org/10.1016/j.teac.2021.e00141.
[21] T.-T. Ma, X.-F. Shen, C. Yang, H.-L. Qian, Y.-H. Pang, X.-P. Yan, Covalent immobilization of covalent organic framework on stainless steel wire for solid-phase microextraction GC-MS/MS determination of sixteen polycyclic aromatic hydrocarbons in grilled meat samples, Talanta J 201 (2019) 413–418, https://doi.org/10.1016/j.talanta.2019.04.031.
[22] N.N. Naing, C.S. Tan, K.H. Lee, Micro-solid-phase extraction 16, Solid-Phase Extr 443 (2019).
[23] M. Sharifi-Rad, M. Kaykhaii, M. Khajeh, A. Oveisi, Synthesis, characterization and application of a zirconium-based MOF-808 functionalized with isonicotinic acid for fast and efficient solid phase extraction of uranium (VI) from wastewater before its spectrophotometric determination, BMC Chem 16 (2022) 27, https://doi.org/10.1186/s13065-022-00821-1.
[24] K. Massoud, H.S. Hashemi, Miniaturized solid phase extraction, In Emerging freshwater pollutants J Elsevier (2022) 49–61, https://doi.org/10.1016/B978-0-12-822850-0.00010-7.
[25] A.A. Asgharinezhad, H. Ebrahimzadeh, A novel polymer coated magnetic porous carbon nanocomposite derived from a metal-organic framework for multi-target environmental pollutants preconcentration, J. Chromatogr. A 1634 (2020) 461664, https://doi.org/10.1016/j.chroma.2020.461664.
[26] N. Heydari, E. Ghorbani-Kalhor, A.A. Asgharinezhad, M. Bahram, M. Taghi Vardini, Determination of phthalate esters in real matrixes after extraction with a novel magnetic nano-material derived from a metal–organic framework, Microchem. J. 191 (2023) 108704, https://doi.org/10.1016/j.microc.2023.108704.
[27] A.A. Asgharinezhad, H. Ebrahimzadeh, Magnetic porous carbon nanocomposite derived from cobalt based-metal-organic framework for extraction and determination of homo and hetero-polycyclic aromatic hydrocarbons, Talanta 233 (2021) 122526, https://doi.org/10.1016/j.talanta.2021.122526.
[28] M. Kaykhaii, H.S. Hashemi, J. Gębicki, Applications of metal organic framework adsorbents for pipette-tip micro solid-phase extraction, TrAC - Trends Anal. Chem 179 (2024) 117877, https://doi.org/10.1016/j.trac.2024.117877.
[29] J. Woźniak, J. Nawała, D. Dziedzic, S. Popiel, Overview of Liquid Sample Preparation Techniques for Analysis Using Metal-Organic Frameworks as Sorbents 29 (2024) 4752, https://doi.org/10.3390/molecules29194752.
[30] S. Moinfar, A. Khodayari, S.S. Abdulrahman, A. Aghaei, S. Sohrabnezhad, L. A. Jamil, Development of a SPE/GC–MS method for the determination of organophosphorus pesticides in food samples using syringe filters packed by GNP/MIL-101 (Cr) nanocomposite, Food Chem. 371 (2022) 130997, https://doi.org/10.1016/j.foodchem.2021.130997.
[31] T. Chen, D. Zhao, Post-synthetic modification of metal-organic framework-based membranes for enhanced molecular separations, Coord. Chem. Rev. 491 (2023) 215259, https://doi.org/10.1016/j.ccr.2023.215259.
[32] X. Zhao, X. Miao, Metal− organic framework constructed by flexible ligands: A versatile platform towards efficient fluorescence sensing, adsorption separation, and heterogeneous catalysis, Coord. Chem. Rev. 502 (2024) 215611, https://doi.org/10.1016/j.ccr.2023.215611.
[33] H. Martínez-Pérez-Cejuela, M. Guiñez, E.F. Simó-Alfonso, P. Amorós, J. El Haskouri, J.M. Herrero-Martínez, In situ growth of metal-organic framework HKUST-1 in an organic polymer as sorbent for nitrated and oxygenated polycyclic aromatic hydrocarbon in environmental water samples before quantitation by

HPLC-UV, Microchim. Acta 187 (2020) 1–9, https://doi.org/10.1007/s00604-020-04265-z.
[34] Y. Lv, X. Tan, F. Svec, Preparation and applications of monolithic structures containing metal–organic frameworks, J. Sep. Sci. 40 (2017) 272–287, https://doi.org/10.1002/jssc.201600423.
[35] F. Maya, C.P. Cabello, A. Figuerola, G.T. Palomino, V. Cerdà, Immobilization of metal–organic frameworks on supports for sample preparation and chromatographic separation, Chromatographia 82 (2019) 361–375, https://doi.org/10.1007/s10337-018-3616-z.
[36] F. Rezaei, Shane Lawson, Hooman Hosseini, Harshul Thakkar, Amit Hajari, Saman Monjezi, A. Rownaghi Ali, MOF-74 and UTSA-16 film growth on monolithic structures and their CO2 adsorption performance, Chem. Eng. J. 313 (2017) 1346–1353, https://doi.org/10.1016/j.cej.2016.11.058.
[37] A. Saeed, F. Maya, D.J. Xiao, M. Najam-ul-Haq, F. Svec, D.K. Britt, Growth of a highly porous coordination polymer on a macroporous polymer monolith support for enhanced immobilized metal ion affinity chromatographic enrichment of phosphopeptides, Adv. Funct. Mater. 5790 (2014) 5797, https://doi.org/10.1002/adfm.201400116.
[38] N. Chang, Z.-Y. Gu, H.F. Wang, X.-P. Yan, Metal-organic-framework-based tandem molecular sieves as a dual platform for selective microextraction and high-resolution gas chromatographic separation of n-alkanes in complex matrices, Anal. Chem.J 83 (2011) 7094–7101, https://doi.org/10.1021/ac2014004.
[39] M.G. Kochameshki, A. Marjani, M. Mahmoudian, K. Farhadi, Grafting of diallyldimethylammonium chloride on graphene oxide by RAFT polymerization for modification of nanocomposite polysulfone membranes for use in water treatment, Chem. Eng. J. 309 (2017) 206–221, https://doi.org/10.1016/j.cej.2016.10.008.
[40] O.S. Serbanescu, S.I. Voicu, V.K. Thakur, Polysulfone functionalized membranes: properties and challenges, Mater. Today Chem. 17 (2020) 100302, https://doi.org/10.1016/j.mtchem.2020.100302.
[41] S.H. Hashemi, F. Keykha, Application of the response surface methodology in the optimization of modified molecularly imprinted polymer-based pipette-tip micro-solid phase extraction for spectrophotometric determination of nicotine in seawater and human plasma, Anal. Methods 11 (2019) 5405–5412, https://doi.org/10.1039/C9AY01496A.
[42] S.H. Hashemi, N. Naruie, Application of response surface methodology for pipette-tip micro solid-phase extraction of nicotine from cigarette, seawater, and human plasma by a novel carbon nanotube/zinc oxide nanocomposite sorbent following its determination by spectrophotometry.J, Anal. Chem. 76 (2021) 563–572, https://doi.org/10.1134/S1061934821050117.
[43] S. Moinfar, A. Khodayari, A.M. Mohammed, E. Pourbasheer, A. Aghaei, NH2-MIL-101 (Cr)/SBA15 nanocomposite as sorbent in syringe-filter-SPE for determination of pesticides in environmental water, Microchem. J. (2025) 115322, https://doi.org/10.1016/j.microc.2025.115322.
[44] S. Moinfar, A. Khodayari, H.Z. Sami, M.K. Ali, L.A. Jamil, Investigation of five metal-organic frameworks as sorbents in the syringe filter-SPE method for the determination of metronidazole and cephalexin in water samples, New J. Chem. 46 (2022) 10308–10316, https://doi.org/10.1039/D2NJ00907B.
[45] H. Fan, A. Gao, G. Zhang, S. Zhao, J. Cui, Y. Yan, A design of bifunctional photothermal layer on polysulfone membrane with enclosed cellular-like structure for efficient solar steam generation, Chem. Eng. J. 415 (2021) 128798, https://doi.org/10.1016/j.cej.2021.128798.
[46] N. Hadi, R. Alizadeh, A. Niaei, Synthesis and characterization of MFI zeolite nanosheets for optimizing the dominant operational conditions of methanol to propylene process, J Nanostructures 9 (2019) 51–73, https://doi.org/10.22052/jns.2018.99008.1612.
[47] S.Y. Chong, T.T. Wang, L.C. Cheng, H.Y. Lv, M. Ji, Metal–organic framework MIL-101-NH_2-supported acetate-based butylimidazolium ionic liquid as a highly efficient heterogeneous catalyst for the synthesis of 3-Aryl-2-oxazolidinones, Langmuir 35 (2018) 495–503, https://doi.org/10.1021/acs.langmuir.8b03153.
[48] E. Haghighi, S. Zeinali, Nanoporous MIL-101 (Cr) as a sensing layer coated on a quartz crystal microbalance (QCM) nanosensor to detect volatile organic compounds (VOCs), RSC Adv. 9 (2019) 24460–24470, https://doi.org/10.1039/C9RA04152D.
[49] X.-L. Wang, H.-L. Fan, Z. Tian, E.-Y. He, Y. Li, J. Shangguan, Adsorptive removal of sulfur compounds using IRMOF-3 at ambient temperature, Appl. Surf. Sci. 289 (2014) 107–113, https://doi.org/10.1016/j.apsusc.2013.10.115.
[50] T. Wang, P. Zhao, N. Lu, H. Chen, C. Zhang, X. Hou, Facile fabrication of Fe3O4/MIL-101 (Cr) for effective removal of acid red 1 and orange G from aqueous solution, Chem. Eng. J. 295 (2016) 403–413, https://doi.org/10.1016/j.cej.2016.03.016.
[51] R. Kumar, A.F. Ismail, M.A. Kassim, A.M. Isloor, Modification of PSf/PIAM membrane for improved desalination applications using Chitosan coagulation media, Desalination 317 (2013) 108–115, https://doi.org/10.1016/j.desal.2013.03.008.
[52] H. Wang, et al., Pr ep rin t n ot pe er re v Pr ep rin t n ot pe er v ed, 2026.
[53] F. Yan, H. Pei, Y. Pei, T. Li, J. Li, B. He, Y. Cheng, Z. Cui, D. Guo, J. Cui, Preparation and characterization of polysulfone-graft-4′-aminobenzo-15-crown-5-ether for lithium isotope separation, Ind. Eng. Chem. Res. 54 (2015) 3473–3479, https://doi.org/10.1021/acs.iecr.5b00314.
[54] D. Nasirian, I. Salahshoori, M. Sadeghi, N. Rashidi, M. Hassanzadeganroudsari, Investigation of the gas permeability properties from polysulfone/polyethylene glycol composite membrane, Polym. Bull. 77 (2020) 5529–5552, https://doi.org/10.1007/s00289-019-03031-3.
[55] X. He, W. Yang, S. Li, Y. Liu, B. Hu, T. Wang, X. Hou, An amino-functionalized magnetic framework composite of type Fe3O4-NH2 MIL-101 (Cr) for the extraction of pyrethroids coupled with GC-ECD, Microchim. Acta. 185 (2018) 125, https://doi.org/10.1007/s00604-018-2672-2.
[56] F.N. Chianeh, J.B. Parsa, Electrochemical degradation of metronidazole from aqueous solutions using stainless steel anode coated with SnO2 nanoparticles: experimental design, J. Taiwan Inst. Chem. Eng. 59 (2016) 424–432, https://doi.org/10.1016/j.jtice.2015.09.019.
[57] E.A. Alenyorege, H. Ma, J.H. Aheto, I. Ayim, F. Chikari, R. Osae, C. Zhou, Response surface methodology centred optimization of mono-frequency ultrasound reduction of bacteria in fresh-cut Chinese cabbage and its effect on quality, Lwt 122 (2020) 108991, https://doi.org/10.1016/j.lwt.2019.108991.
[58] X. Cao, G. Liu, Y. She, Z. Jiang, F. Jin, M. Jin, P. Du, F. Zhao, Y. Zhang, J. Wang, Preparation of magnetic metal organic framework composites for the extraction of neonicotinoid insecticides from environmental water samples.RSC, Adv 6 (2016) 113144–113151, https://doi.org/10.1039/C6RA23759B.
[59] V. Guzsvány, J. Csanádi, F. Gaál, NMR study of the influence of pH on the persistence of some neonicotinoids in water, Acta Chim. Slov. 53 (2006) 52.
[60] E.N. Bakatula, D. Richard, C.M. Neculita, G.J. Zagury, Determination of point of zero charge of natural organic materials, Environ. Sci. Pollut. Res. 25 (2018) 7823–7833, https://doi.org/10.1007/s11356-017-1115-7.
[61] W. Ma, B. Yang, J. Li, X. Li, Amino-functional metal–organic framework as a general applicable adsorbent for simultaneous enrichment of nine neonicotinoids, Chem. Eng. J. 434 (2022) 134629, https://doi.org/10.1016/j.cej.2022.134629.
[62] G. Wu, J. Ma, C. Wei, S. Li, J. Li, X. Wang, L. Chen, Determination of neonicotinoid insecticides in environmental water by the enrichment of MIL-53 mixed matrix membrane coupled with high performance liquid chromatography int, J. Environ. Res. Public Health 20 (2023) 715, https://doi.org/10.3390/ijerph20010715.
[63] M.C. Kreider, et al., Toward 3D printed hydrogen storage materials made with ABS-MOF composites, Polym. Adv. Technol. 29 (2018) (2018) 867–873, https://doi.org/10.1002/pat.4197.
[64] P. Yin, Y. Dong, X. Zhou, Q. Wang, S. Li, C. Wang, L. Hao, Z. Wang, Q. Wu, Synthesis of phosphate-functionalized magnetic porous organic polymer: A sorbent for sensitive determination of neonicotinoid insecticides in water and lemon juice, J. Chromatogr. A 1705 (2023) 464221, https://doi.org/10.1016/j.chroma.2023.464221.
[65] X. Xu, J. Gao, M. Ran, Y. Guo, D. Feng, L. Zhang, Nanoconfinement of functionalized ionic liquid for enhanced adsorption and rapid sensitive detection of phenylurea herbicides in food and environmental samples, Food Chem. 431 (2024) 137149, https://doi.org/10.1016/j.foodchem.2023.137149.
[66] P. Wang, M. Luo, D. Liu, J. Zhan, X. Liu, F. Wang, Z. Zhou, P. Wang, Application of a magnetic graphene nanocomposite for organophosphorus pesticide extraction in environmental water samples, J. Chromatogr. 1535 (2018) 9–16, https://doi.org/10.1016/j.chroma.2018.01.003.
[67] H. Ding, R. Wang, W. Liu, S. Cheng, W. Ji, Z. Zheng, X. Wang, A spherical metal-organic coordination polymer for the microextraction of neonicotinoid insecticides before their determination by HPLC, Microchim. Acta 186 (2019) 2–9, https://doi.org/10.1007/s00604-018-3210.
[68] H. Martínez-Pérez-Cejuela, K. Pravcová, L. Česlová, E.F. Simó-Alfonso, J. M. Herrero-Martínez, Zeolitic imidazolate framework-8 decorated with gold nanoparticles for solid-phase extraction of neonicotinoids in agricultural samples 188, 2021, p. 197, https://doi.org/10.1007/s00604-021-04872-4.